Korean J. Chem. Eng., 34(12), 3102-3110 (2017)
DOI: 10.1007/s11814-017-0217-8

pISSN: 0256-1115
eISSN: 1975-7220

Multilateral approaches for investigation of particle stickiness of coal ash at low temperature fouling conditions

Hueon Namkung*, Hyung-Taek Kim*,,†, Fuchen Wang*, Kuangfei Lin*, and Guangsuo Yu*,†**

*Key Laboratory of Coal Gasification and Energy Chemical Engineering of Ministry of Education, East China University of Science and Technology, Shanghai, 200237, P. R. China
**Department of Energy Systems Research, Graduate School, Ajou University, Woncheon-dong, Yeongtong-gu, Suwon 16499, Korea
(*Received 31 January 2017 • accepted 9 August 2017*)

Abstract−Particle stickiness is a key parameter for increasing ash deposition in gasification process. We conducted multilateral investigations to evaluate particle stickiness of coal ash at low temperature fouling conditions through Watt and Fereday's viscosity model, dilatometry (DIL) and laser flash apparatus (LFA) technique. Seventeen coals were employed for ash deposition experiments under gasification condition through drop tube furnace (DTF). The low viscosity not only led to increasing ash deposition behavior, but also increasing the particle size of deposited ash. From DIL analysis, the ash sintering behavior increased with increasing temperature due to increase of particle stickiness. The high amount of Fe_2O_3, CaO and MgO components resulted in low sintering temperature and high reduction of physical length. Through LFA analysis, the thermal conductivity increased with increasing temperature, because of increasing particle stickiness. In addition, its value was correlated with the propensity of common fouling indices.

Keywords: Ash Fouling, Gasification, Stickiness, Sintering, Thermal Conductivity

INTRODUCTION

Ash-related problems could be a potential concern during thermochemical conversion of coal [1,2]. The release and transformation of inorganic species from reaction and burning of coal with reactants (e.g. oxygen, air and steam) during the thermochemical processes may lead to problems, such as ash fouling on heat transfer surface and slag formation (especially, >1,300 °C) in a reaction furnace [3,4]. In general, alkali and alkaline earth metals among inorganic species are recognized as crucial chemical components for increasing fouling behavior [5]. CaO and MgO lower the softening temperature of ash and lead to increasing particle stickiness [6]. They have been used as chemical parameters in typical fouling indices [6,7]. In addition, Fe_2O_3 has been known for leading to increasing fouling and slagging behavior [8]. Entrained-flow gasification technology is a promising energy conversion way of coal for environment-friendly and efficient usage [9-11]. Fouling behavior can severely occur in a heat exchanger in entrained-flow gasification process, because of high operating temperature. The ash deposition rate is related to the impaction velocity [12,13] and stickiness of particles [14-17] if the type of fuel and experimental conditions (e.g. gasification/deposition temperature, structure of deposition target, material roughness and physicochemical properties of fuel) are the same. In particular, the stickiness of particles is a dominant parameter to determine the ash deposition behavior [18]. When the ash particles arrive at the deposition target, they can undergo three different movements: removal (the mechanism for decay), rebounding (bilateral mechanism for growth and decay) and adhesion (the mechanism for growth) according to particle stickiness [19].

If particles are sintered by sticky characteristic on the deposit, these behaviors increase the deposition possibility of dropped particles. This means that sintered particles, which contain partial liquid surface, reduce removal force after the collision to escape from the deposit target. As a result, sintered particles on the deposited layer encourage fouling growth.

Abd-Elhady et al. [20] and Pan et al. [21] investigated the removal propensity and critical sticking criterion according to the characteristics of the deposited layer. Abd-Elhady et al. recorded an image of the dropped particle on the fouling layer. In the recorded image, two different types of behaviors are measured such as rebounding (relocation of particles) and removal (escape of particles from deposition target). These movements differ depending on whether it is a sintered or particulate layer. They measured the number of ejected particles from deposition target at different impacting particle velocities according to the characteristics of the deposited layer. The number of ejected particles was found to increase with increasing impacting velocity on the particulate layer. However, the number of ejected particles on the sintered layer is comparatively small even when the impacting velocity increases.

Pan et al. investigated the fouling growth rate according to the relation between porosity and the impacting velocity. They simulated fouling growth by a numerical method. According to their results, the critical rebounding (i.e., removal) velocity, which causes dropped particles to escape from the deposition target after collision, increases with increasing porosity of the fouling layer, but oth-

†To whom correspondence should be addressed.
E-mail: gsyu@ecust.edu.cn, htkim@ajou.ac.kr
‡5th International Conference on Gasification and Its Application.

erwise decreases. So even when the impacting velocity of particles is high, the deposition rate of dropped particles may increase on a sintered fouling layer due to low porosity.

As mentioned in previous researches, the stickiness might enable changes of sintering and thermal conductivity of deposited ash. To study sintering and thermal conductivity, dilatometer (DIL) and laser flash apparatus (LFA) were utilized, respectively. DIL is a useful technique for investigating the sintering behavior of solid material. The sintering behavior of ash at high temperatures has been researched through DIL to clarify the particle transformation [22-25]. The sintering rate is determined by measuring the changes in physical length of a pellet. Meanwhile, the physical and chemical property of ash fouling influence the heat transfer efficiency at the heat exchanger. Many previous researchers investigated the thermal conductivity of ash deposits [26-28]. However, the experimental method and apparatus varied in those studies and resulted in unstandardized data. LFA is a very typical instrument for studying thermal conductivity of the solid particles [29-31].

In this study, we used seventeen samples in range of bituminous and sub-bituminous coal for laminar-flow drop tube furnace (DTF) experiments. The deposition ratio (Deposit fouling/Input ash) was fitted with sticking efficiency based on traditional viscosity equation such as Watt and Fereday model [32] and then their relation was assessed. To clarify the particle stickness by change of sintering bahavior at different temperatures and chemical factor affecting in sintering temperature and reduction of sample length, DIL analysis was carried out. In addition, LFA analysis was attempted to evaluate change of particle stickiness through investigating the relation between themal conductivity and fouling indices based on chemical components.

EXPERIMENTAL SECTION

1. Experimental Samples

Seventeen different coal samples were chosen for the experiments, which represented a wide range of mineral content of bituminous and sub-bituminous coal. The basic properties of the coal samples were measured by proximate and ultimate analysis, and the chemical compositions and fusion temperatures of the coal ash samples were also analyzed. The properties of bituminous coal and sub-bituminous coal are listed in Table 1. The original coal samples were dried and crushed in a fan-type disk mill, and then separated below 75 μm and 150 μm. All of the particle samples were dried in an electric oven at 60 °C for 24 h before the experiments.

2. Experimental Facility and Method

2-1. DTF

The DTF, where the laminar flow can be made, is a lab scale coal entrained-flow gasifier. The system components mainly consisted of a coal sample injector, pre-heater, main reactor and ash collector. A detailed schamtic diagram and ash collector of DTF are expressed in previous works in detail [33-35]. The ash deposition experiments were coducted under gasification environment. First, the surface temperature of the ash collector was set to 700 °C in DTF before starting the experiment. After then, coal separated below 75 μm and O_2 gas were introduced into the DTF. Each experiment time was set to 10 min. During experiments, coal and O_2 gas were continuously injected into the DTF for ash deposition (feeding rate of coal: about 0.5 g/min, the equivalent ratio of O_2/coal: 0.9). After the experiment, the ash deposited on the collector was detached and then its total weight was measured by using an electronic balance. To measure the particle size of deposited ash, the particle size analyzer (Malvern mastersizer 2000) was also employed.

2-2. DIL

Seven ash samples were prepared in the muffle furnace. For preparation of the ash samples, pulverized coal samples, in which the particle sizes were below 150 μm, were heated at 815 °C for 2.5 h. The powdery ash of 0.3-0.4 g prepared by adding 10 wt% of a polyvinyl alcohol (PVA) solution was used. The ash samples for DIL analysis were prepared by pressing at 3.5 bars, and then the compressed and pelletized ash samples were loaded into the DIL. The size of each pelletized ash sample was about ø 6.5 mm (diameter)×8 mm (length). The actual physical length variation of the ash samples was measured in the DIL. The temperature in the DIL was increased with 20 °C/min heating rate from room temperature to 700, 800 and 900 °C under Ar environment, respectively, and then the reactions were maintained under isothermal conditions for 3 h, because low temperature fouling generally occurs below 1,000 °C.

From the results of DIL analysis, reduction of physical length could be calculated during isothermal sintering conditions.

2-3. LFA

LFA has been used to measure thermal conductivity of different materials. In this study, the thermal conductivities of the adopted ash samples were calculated by multiplication of the thermal diffusivity, bulk density, and specific heat of the samples. The equation for calculation of the thermal conductivity is shown as follows:

$$\lambda = \alpha \rho C_p \quad (1)$$

where,
λ: Thermal conductivity (W/m·K)
α: Thermal diffusivity (mm^2/sec)
ρ: Bulk density (g/cm^3)
C_p: Specific heat (J/g·K)

Experimentally, the thermal conductivity measurements were performed as follows. First, coal particles sized below 150 μm were separated and treated at 815 °C for ashing after which the ash samples were pelletized at 400 bar. The size of the pellets, which have the shape of a circular plate, is about 1 mm (height)×10 mm (diameter). Before starting the LFA analysis, the bulk density of sample pellet was measured. In the case of thermal diffusivity and specific heat of the sample, the value was measured during LFA analysis as a fucntion of temperature.

RESULTS AND DISCUSSION

1. Effect of Viscosity for Ash Deposition and Particle Size

Stickiness is an important factor for ash deposition. If ash particles have sticky characteristics, they can be capable for deposition and capture possibility for non-sticky particles. Therefore, sticky particles can be expected to lead to increased ash deposition and

Table 1. Basic properties of experimental samples

		Bituminous coal										Sub-bituminous coal						
		Datong	Cyprus	Denisovsky	Shenhua	Zhongmei	Minmetal	Taldinsky (1)	Taldinsky (2)	Bengalla	WH	MSJ	Usibelli	Roto	MHU	KPU	LG	ABK
Proximate analysis (dry-basis, wt%)	V.M	33.52	46.64	25.81	31.83	26.77	29.01	32.32	29.58	36.72	32.13	51.29	48.19	46.52	46.3	55.62	53.38	42.39
	F.C	57.36	47.3	60.98	57.57	64.15	61.57	55.67	56.73	44.76	48.67	42.82	41.75	50.2	48.71	38.58	38.21	50.83
	Ash	9.12	6.06	13.19	10.6	9.08	9.42	12.01	13.69	18.51	19.2	5.91	10.06	3.28	4.99	5.8	8.42	6.78
Ultimate analysis (dry ash-free, wt%)	C	73.86	68.22	85.6	77.67	82.91	85.06	79.59	88.52	83	87.99	75.61	63.56	66.99	59.71	76.11	76.66	74.12
	H	4.75	5.25	5.16	4.4	4.05	4.75	4.74	5.29	5.39	5.7	5.36	5.32	4.49	4.61	5.28	5.39	5.39
	O	20	24.55	7.75	16.57	11.26	8.48	13.53	2.97	8.62	3.05	15.78	30.17	27.44	33.33	16.79	15.26	17.98
	N	0.73	1.19	1.13	0.29	0.74	0.79	1.94	2.54	1.9	1.94	1.79	0.75	0.97	1.31	1.27	1.55	1.44
	S	0.66	0.79	0.36	1.07	1.04	0.92	0.2	0.68	1.09	1.32	1.47	0.2	0.11	1.04	0.49	1.05	0.52
Heating value (HHV)	kcal/kg	7,386	6,822	7,139	6,785	6,885	6,601	6,814	7,069	6,165	6,628	6,812	5,304	6,154	5,706	6,570	6,539	6,325
Inorganic analysis (wt%)	SiO_2	55.16	62.29	55.36	45.51	60.08	42.9	42.2	60.51	58.73	55.44	44.23	45.1	37.49	29.2	36.63	49.94	44.42
	Al_2O_3	19.07	16.89	26.74	17.18	25.74	11.2	14.1	27.59	27.86	31.39	28.66	19.98	16.46	9.26	20.79	29.24	23.73
	Fe_2O_3	13.18	7.19	8.41	10.89	7.44	19.7	24.9	5.14	5.85	4.44	11.21	6.33	19.32	46.2	7.99	8.56	12.85
	CaO	8.53	8.34	4.45	21.49	3.78	17.3	9.15	2.26	4.85	5.24	6.94	22.18	17.46	8.62	19.42	5.41	11.73
	MgO	1.23	2.16	1.92	1.55	0.49	0.34	0.33	1.44	1.21	0.71	3.15	3.3	7.23	0.16	6.06	2.83	3.64
	Na_2O	0.64	1.1	0.41	1.5	0.57	0.06	0.07	0.46	0.49	0.29	2.78	0.98	0.09	-	6.58	1.42	1.29
	K_2O	1.4	1.1	1.71	1.1	1.03	4.18	4.67	1.79	0.68	0.71	1.9	1.34	0.91	3.31	1.57	2.01	1.46
	TiO_2	0.78	0.93	1	0.78	0.87	4.32	4.59	0.75	0.68	1.53	0.92	0.78	1.04	3.17	0.78	0.94	0.86
Ash fusion temp. (^oC)	Fluid	1,308	1,289	1,400	1,258	1,421	1,310	1,360	>1,450	1,356	1,412	1,310	1,257	1,270	1,310	1,220	1,388	-

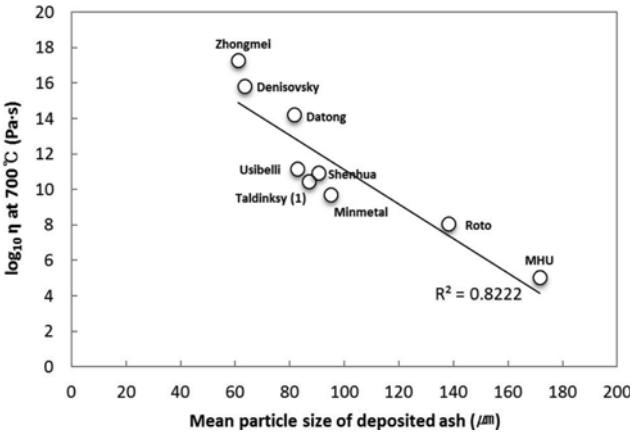

Fig. 1. Relationship between viscosity and mean particle size of deposited ash at 700 °C.

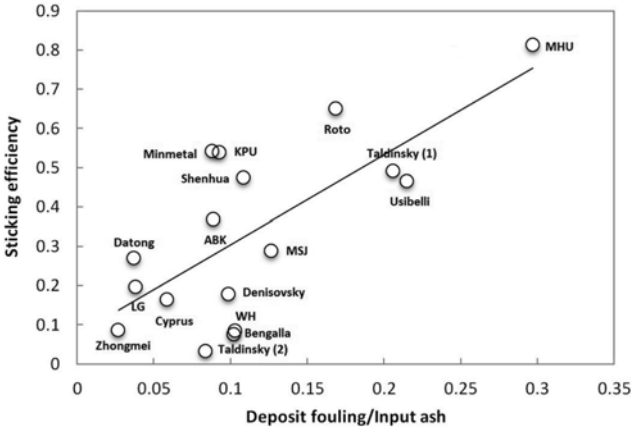

Fig. 2. Relationship between sticking efficiency and ash deposition ratio.

sintering behavior. Previous researchers studied critical viscosity affecting ash deposition and sintering behavior [36-38]. According to their study, the critical viscosity ranged from 10^7 to 10^9 Pa·s for initial ash deposition and sintering. The measurement of ash viscosity at ash deposition temperature is difficult, because the state of the ash is not formed as a liquid. Normally, it is possible to calculate the viscosity under low-temperature fouling conditions by using the representative viscosity model (e.g., Urbain and Watt & Fereday models). We used the Watt & Fereday model to calculate the ash viscosity as a function of temperature.

The stickiness could influence the size growth of ash particles as well as the ash deposition rate, because it leads to agglomeration among ash particles. The relationship between the particle size of deposited ash of different types of coal and their viscosity was compared at 700 °C (Fig. 1). Before the particle size analysis, deposited ash collected after the DTF experiment was pre-treated by electromagnetic shaking to separate the physically agglomerated ash particles to enable the particle size to be analyzed accurately. The particle size of deposited ash was measured at least ten times to calculate the mean particle size, and it was found that the lower the viscosity value, the larger the mean particle size. Even though the initial particle size of coal introduced into the DTF was below 75 μm, the sizes of some of the particles of the deposited ash exceeded those of the input coal particle. The ash particle sizes of Roto and MHU coal, including the high alkaline earth and alkali metals, were larger than those of the other samples, because of their low viscosity values.

Particles having viscosities lower than the critical viscosity could possibly adhere directly to the deposition target. Depending on the viscosity values, the possibility of ash deposition can be expressed in terms of the "sticking efficiency" [39]. The calculation method of sticking efficiency is shown as follows.

- Sticking efficiency

$$(\eta_{cv} - \eta_T)/\eta_{cv} \quad (2)$$

where,

η_{cv}: Critical viscosity (10^9 Pa·s)

η_T: Viscosity at given temperature (Pa·s)

The critical viscosity was chosen as 10^9 Pa·s, because, according to previous literature report, this value is necessary to ensure minimum particle sticking behavior. The relation of ash deposition ratio and sticking efficiency is fitted in Fig. 2. High sticking efficiency led to increasing ash deposition ratio, because low viscosity resulted in high sticking efficiency. Even though the ash was collected at 700 °C through DTF experiment, the viscosity value calculated at 900 °C was adopted for sticking efficiency. Most viscosity values calculated at 700 °C were higher than critical viscosity (10^9 Pa·s). If the viscosity value presents higher than critical viscosity, it does not have sticky characteristic. On the other hand, the viscosity calucated by Watt and Fereday model at 900 °C met the critical viscosity. In addition, the DIL results showed that the sintering temperature of ashes was mostly found between 800 °C and 900 °C. In particular, sintering behavior at 900 °C was higher than other temperatures (section 2). According to the fouling growth mechanism [40], the temperature of the intermediate layer of deposited fouling is higher than that at the surface of the deposit, because of the insulation effect of the fouling layer. In the intermediate stage, fouling growth may be rapid as a result of increasing stickiness at that stage. The temperature of the inner fouling layer may range from 700 °C (surface temperature) to 1,300 °C (flue gas temperature). Therefore, the value of the sticking efficiency at 900 °C can be adopted to compare the ash deposition ratio.

2. Effect of Sintering Behavior by Particle Stickiness

The sintering phenomenon of ash particle in commercial entrained-flow gasification process is very complicated to explain its behavior, because the deposition phenomenon might be generated by both fly ash and slag. Therefore, solid phase and liquid phase sintering phenomenon can co-occur on deposition target. In general, the sintering mechanism between them is different. In the case of solid phase sintering, atoms on particles move to the neck interface of particles. On the other hand, in the case of liquid phase sintering, the liquid spreads around the solid phase particles for the sintering. The liquid may provide for rapid transport and result in rapid sintering if certain criteria are met. The sintering behavior on liquid phase is more rapid than on solid phase [41].

If liquid phase materials are adhering on the deposit surface,

most of the dropped particles might be deposited. At that condition, particle characteristics such as sticking and non-sticking are meaningless for studying fouling phenomena. It is important to know the critical factor in fouling deposition related to stickiness. Thus, in this study, solid phase sintering is only considered. To measure the physical length variation of ash by sintering under isothermal condition, the DIL temperature was set to 700, 800 and 900 °C, respectively. The sample was injected into the DIL at room temperature, after which the temperature was increased at the fastest heating rate (20 °C/min) up to the desired temperature. The

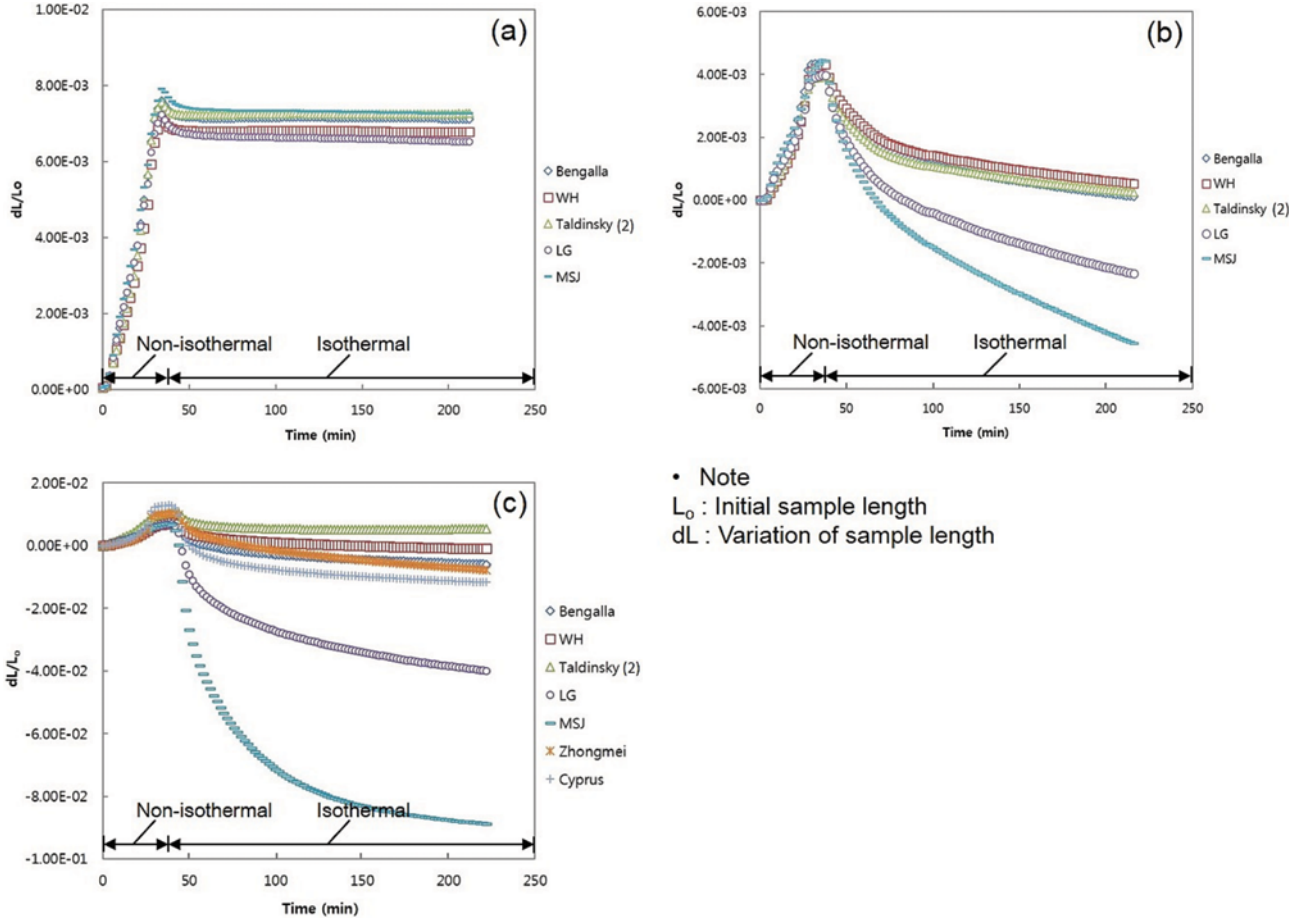

Fig. 3. Length variation of ash pellet under different isothermal conditions ((a) 700 °C, (b) 800 °C and (c) 900 °C).

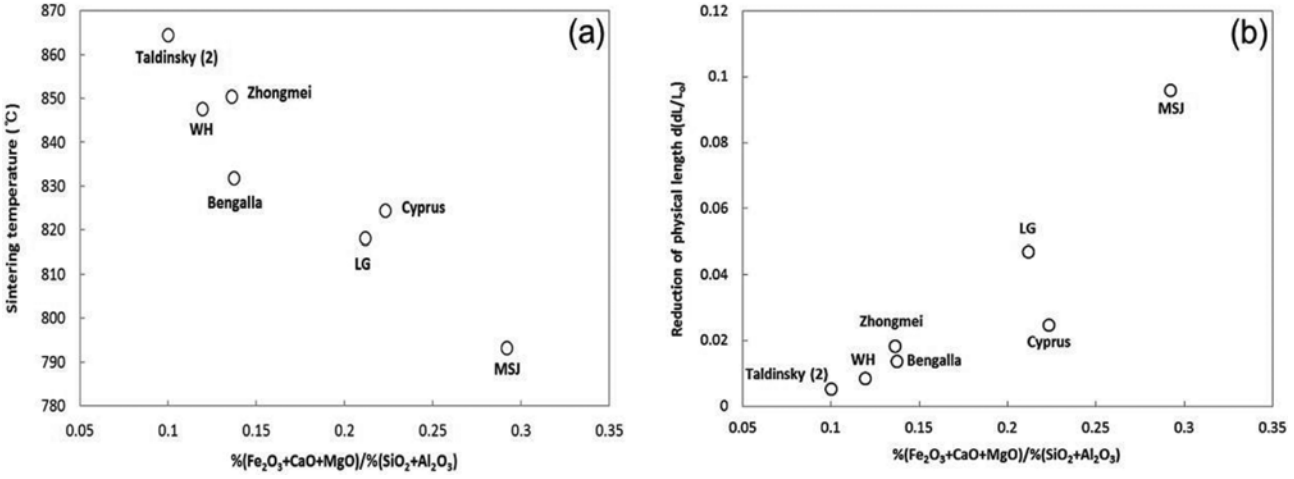

Fig. 4. Chemical effect for sintering temperature and reduction of physical length ((a) effect for sintering temperature and (b) effect for reduction of physical length).

isothermal reaction time of the DIL was set to 3 h. The physical length variation of ash under non-isothermal conditions was ignored when the reduction of physical length was calculated during the sintering process. Reduction of physical length indicates the difference (i.e., densification rate) of the sample length from the highest dL/L_o level to the lowest dL/L_o level.

Fig. 3 shows the variation of physical length under different isothermal conditions, plotted as a function of time. The reduction of physical length was higher at high temperature. The reduction of physical length was not generated at 700 °C. As the possibility of stickiness increases with increasing reaction temperature, reduction of physical length may increase at higher temperatures. Furthermore, the reduction of physical length of ashes was different in spite of the temperature being the same. The reduction of physical length is normally related to the chemical components, i.e., the concentrations of alkali and alkaline earth metals involved. Fig. 4 indicates chemical effect for sintering temperature and reduction of physical length. Sintering occurred after end of the thermal expansion (i.e., the highest dL/L_o level). The sintering temperature indicates the temperature of first decreasing point from the final thermal expansion point. The sintering temperature of ash containing high amount of Fe_2O_3, CaO and MgO components was low. The physical length variation of the MSJ and LG ashes, which have a high alkali and alkaline earth metal content, is higher than that of the others. In particular, Fe_2O_3, CaO and MgO components lead to an increase in the reduction of physical length. High amount of Fe_2O_3, CaO and MgO enables to influence the stickiness of ash particle, because sintering behavior is related to those chemical components.

3. Relation of Thermal Conductivity and Fouling Indices Based on Chemical Components

Particles having stickiness affect the thermal conductivity of ash deposit as well as sintering behavior. In general, the thermal conductivity of the ash deposit varies by the porosity, chemical components, and physical state of deposited ash and deposit temperature. The variation of thermal conductivity is resultingly indicated as a function of particle stickiness. The chemical components influencing the porosity and physical structure of the ash deposit are key parameters for transformation of particle stickiness. In previous research [42,43], the thermal conductivities of pure and mixed oxides and coal ashes were investigated. The results show the thermal conductivity containing high ratios of Al_2O_3 decreases with increasing temperature, whereas the thermal conductivity containing high ratios of SiO_2 increases with increasing temperature. The silica ratio has been reported to be important at high temperature, at which strong sintering and fusion reactions such as slagging state can occur [44]. However, as the melting temperature of silica is very high (1,600 °C), this effect may not be critical under low temperature fouling conditions. Iron-rich deposits, which have low sintering temperatures compared to deposits that are iron deficient [37], may increase the thermal conductivity. The reduction of deposit porosity by sintering leads to an increase in the thermal conductivity of coal ash. Therefore, it is clear that the thermal conductivity of sintered ashes is higher than that of powdery ashes [45].

The thermal conductivities of the sample ashes were compared to the reference data [46] irrespective of whether the data could be considered reliable (Fig. 5). Although the absolute values of the thermal conductivities are not the same, the thermal conductivities of the different ashes exhibit a similar increasing trend. The thermal conductivity of KPU, ABK and MSJ coal containing high amounts of alkali and alkaline earth metals is higher than that of the other coals. In general, alkali and alkaline earth metals can lower the melting temperature, which generates the sintering behavior and decreases the porosity of the structure. The experimental environments (temperature, pressure at which the pellet was

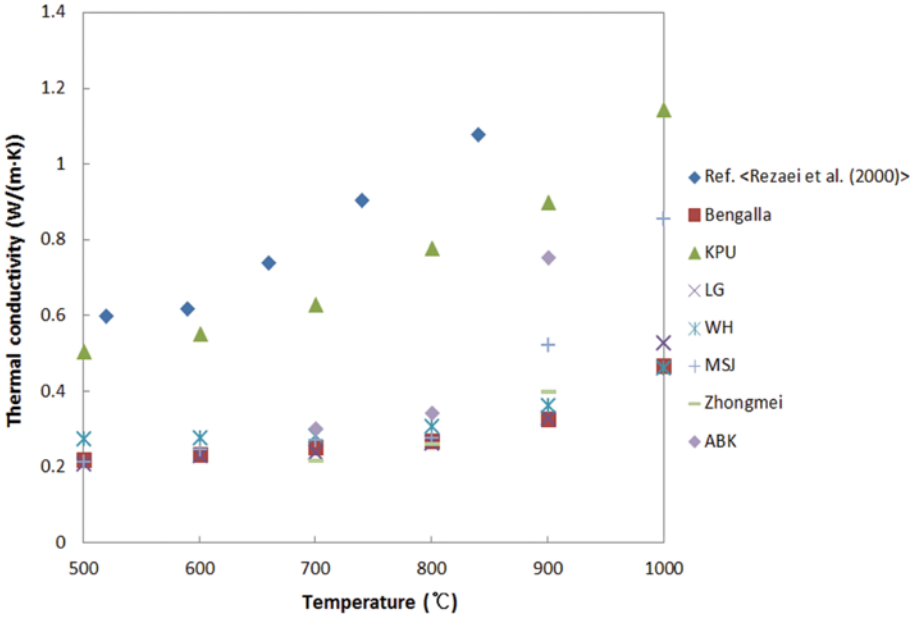

Fig. 5. Thermal conductivities of ashes compared Rezaei et al. [46].

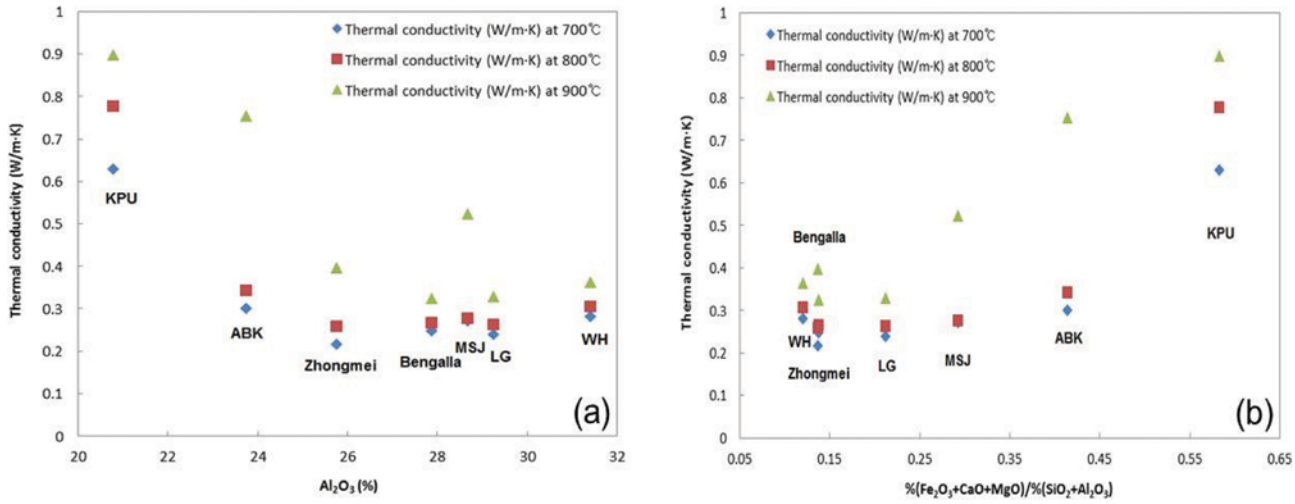

Fig. 6. Relationship between thermal conductivity and chemical components ((a) Al_2O_3 and (b) %(Fe_2O_3+CaO+MgO)/%(SiO_2+Al_2O_3)).

compressed, and sample size), in which the thermal conductivity of the different samples was measured, were similar. Therefore, the thermal conductivities were compared as a function of the chemical components. The relationship between the thermal conductivity and the Al_2O_3 ratio of ash is compared in Fig. 6(a).

The thermal conductivity of the ashes decreases with increasing Al_2O_3 ratio, because Al_2O_3 is one of the acidic metal components, which generally increases the melting temperature. Therefore, in a sample with a high Al_2O_3 content, the ash particles would not be able to undergo sintering with each other at the given temperature. In our previous research, Fe_2O_3, CaO, and MgO components were found to be important parameters in fouling growth, because they may lower the melting temperature of ashes. The relationship between thermal conductivity and the %(Fe_2O_3+CaO+MgO)/%(SiO_2+Al_2O_3) ratio is compared in Fig. 6(b). The thermal conductivity of KPU, ABK and MSJ ash, all of which have a high alkali and alkaline earth metal content, is higher compared to the other types of ash. Further, the thermal conductivities of ashes were found to increase with increasing %(Fe_2O_3+CaO+MgO)/%(SiO_2+Al_2O_3) ratio. The ash deposition rate can be predicted by fouling indices based on the chemical components. The chemical components influence both ash deposition and thermal conductivity. Therefore, the thermal conductivity of ashes might be comparable to the fouling indices based on the chemical components. Depending on the propensity for ash deposition, the fouling indices can be divided into low, medium, high, and severe stages shown in Table 2 [47]. According to this criterion, the fouling propensity can be predicted. Fig. 7 indicates the relationship between thermal conductivity and fouling indices based on chemical components.

Table 2. Criteria of fouling propensity in common slagging and fouling indices [47]

	Slagging and fouling propensity			
	Low	Medium	High	Severe
B/A ratio	<0.4 or >0.7		0.4 to 0.7	
Fe_2O_3/CaO	<0.3 or >3.0	0.3 to 3.0		
Fe_2O_3+CaO	<10%	-	-	-
Silica percentage	72%-80%	65%-72%		50%-65%

The base to acid (B/A) ratios of KPU and ABK ash are ranked high and have a severe fouling propensity according to the criterion of fouling indices in Table 2. Their thermal conductivities are also higher than those of the other samples. According to the fouling propensity criterion of Fe_2O_3/CaO ratio in Table 2, all of the measured samples have a high fouling propensity. In particular, the fouling propensity of KPU and ABK may be severe with high thermal conductivity among the samples. In the case of Fe_2O_3+CaO, WH has the lowest thermal conductivity among the samples. This result is also related to the fouling propensity. If the value of Fe_2O_3+CaO is below 10% (Table 2), the fouling propensity is lower. On the other hand, the KPU, ABK and MSJ ash have high thermal conductivities with a high ratio of Fe_2O_3+CaO. In case of comparison between silica percentage and thermal conductivity, the thermal conductivity decreases with increasing silica percentage. Also, fouling propensity decreases with increasing silica percentage. Therefore, the thermal conductivity trends agree with criterion of fouling propensity in indices based on the chemical components. Both the ash deposition rate and thermal conductivity increase with high particle stickiness.

CONCLUSIONS

In an entrained-flow gasification process, the problem of ash deposition is an important issue to ensure continuous plant operation. Ash deposition is mainly related to the stickiness of coal ash. To investigate the particle stickiness at low temperature fouling conditions, multilateral approaches were conducted with DIL and LFA analysis. The chemical components were found to be mainly responsible for the particle stickiness, because they influenced the viscosity, possibility of the ash deposition and sintering/agglomeration behavior as well as structure transformation of deposited ash. The deposition ratio of seventeen coal ashes increased with low viscosity. From DIL analysis, Fe_2O_3, CaO and MgO components

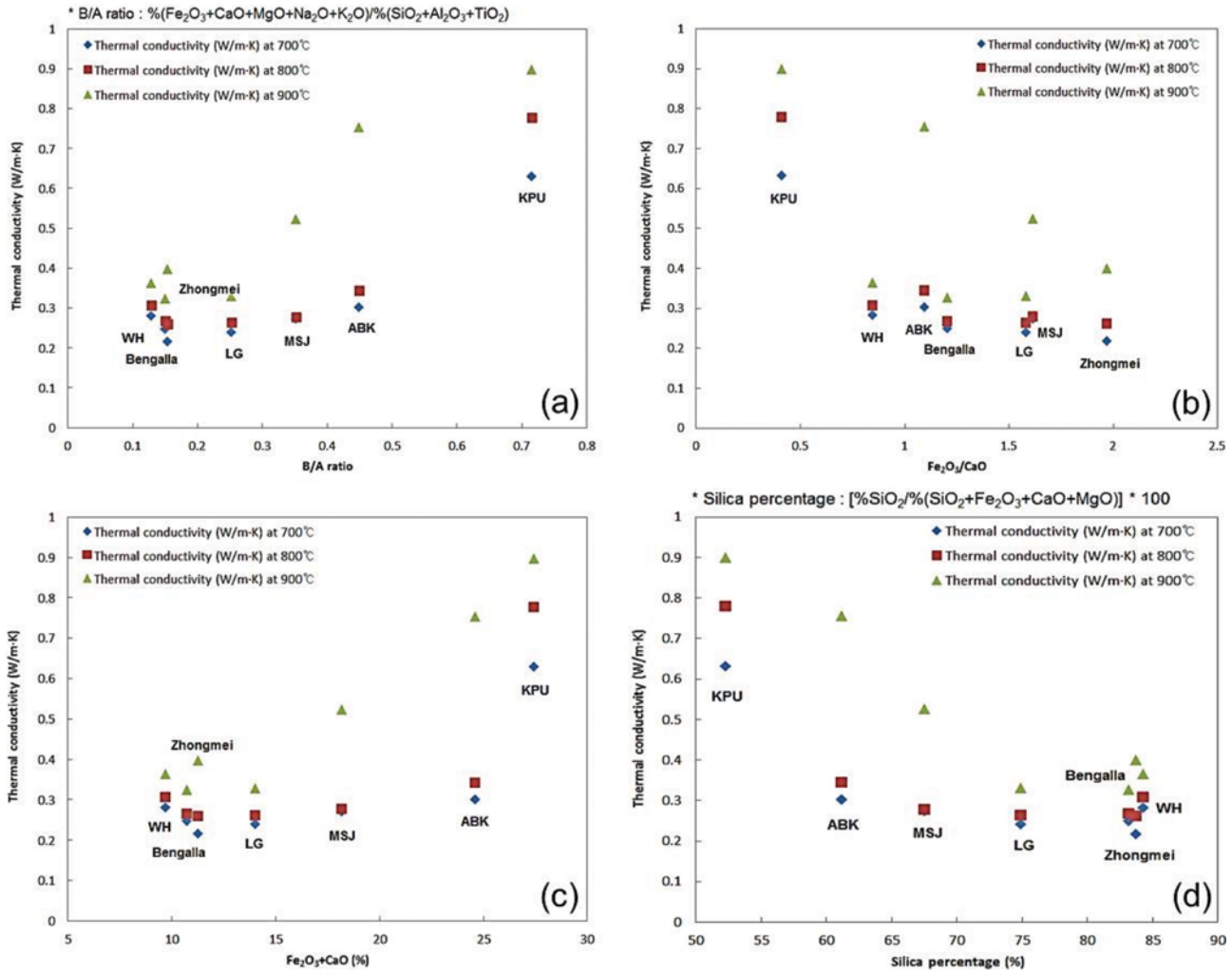

Fig. 7. Relationship between thermal conductivity and fouling indices based on chemical components ((a) B/A, (b) Fe_2O_3/CaO, (c) Fe_2O_3+CaO and (d) Silica percentage).

led to reducing the sintering temperature and raising the reduction of physical length under isothermal sintering process. Furthermore, the thermal conductivity trend agreed with fouling propensity of traditional fouling indices based on chemical components. From this study, we clarified that Fe_2O_3, CaO and MgO components influenced the particle stickiness. As a result, they affected the sintering behavior and thermal conductivity of ash.

ACKNOWLEDGEMENTS

This work was supported by the National Natural Science Foundation of China (21676091) and supported by Sino-Korea Young Scientist Exchange Program (KR-15-03).

REFERENCES

1. F. H. Li, X. W. Ma, Q. Q. Guo, H. L. Fan, M. L. Xu, Q. H. Liu and Y. T. Fang, *Fuel Process. Technol.*, **152**, 124 (2016).
2. X. Wu, X. Zhang, B. Dai, X. Xu, J. Zhang and L. Zhang, *Fuel Process. Technol.*, **152**, 176 (2016).
3. B. Q. Dai, X. Wu, A. D. Girolamo and L. Zhang, *Fuel*, **139**, 720 (2015).
4. P. M. Walsh, *Energy Fuels*, **6**, 709 (1992).
5. L. H. Xu, H. Namkung, H. B. Kwon and H. T. Kim, *J. Ind. Eng. Chem.*, **15**, 98 (2009).
6. J. G. Singer, *Combustion fossil power systems*, in: Combustion Engineering inc, 3rd Ed., Rand McNally, New York (1981).
7. S. Su, J. H. Pohl and D. Holcombe, *Fuel*, **82**, 1653 (2003).
8. S. Vargas, F. J. Frandsen and K. Dam-Johansen, *Prog. Energy Combust. Sci.*, **27**, 237 (2001).
9. S. Lin, L. Ding, Z. Zhou and G. Yu, *Fuel*, **186**, 656 (2016).
10. J. Ni, Z. Zhou, G. Yu, Q. Liang and F. Wang, *Ind. Eng. Chem. Res.*, **49**, 12302 (2010).
11. H. Namkung, X. Hu, H. T. Kim, F. Wang and G. Yu, *Fuel Process. Technol.*, **149**, 195 (2016).
12. J. M. Grillot and G. Icart, *Exp. Therm. Fluid Sci.*, **14**, 442 (1997).
13. H. Müller-Steinhagen, F. Reif, N. Epstein and A. P. Watkinson, *Can. J. Chem. Eng.*, **66**, 42 (1988).
14. J. Barroso, J. Ballester, L. M. Ferrer and S. Jiménez, *Fuel Process. Technol.*, **87**, 737 (2006).

15. Z. Ma, F. Iman, P. Lu, R. Sears, L. Kong, A. S. Rokanuzzaman, D. P. McCollor and S. A. Benson, *Fuel Process. Technol.*, **88**, 1035 (2007).
16. K. Strandström, C. Mueller and M. Hupa, *Fuel Process. Technol.*, **88**, 1053 (2007).
17. S. Li, Y. Wu and K. J. Whitty, *Energy Fuels*, **24**, 1868 (2010).
18. S. Li and K. J. Whitty, *Energy Fuels*, **23**, 1998 (2009).
19. H. Namkung, L. H. Xu, C. H. Kim, X. Yuan, T. J. Kang and H. T. Kim, *Fuel Process. Technol.*, **141**, 82 (2016).
20. M. S. Abd-Elhady, S. H. Clevers, T. N. G. Adriaans, C. C. M. Rindt, J. G. Wijers and A. A. van Steenhoven, *Int. J. Heat Mass Transfer*, **50**, 196 (2007).
21. Y. Pan, F. Si, Z. Xu and C. E. Romero, *Powder Technol.*, **210**, 150 (2011).
22. E. Raask, *J. Thermal Anal.*, **16**, 91 (1979).
23. E. Raask, *Coal ash sintering model and the rate measurements*, Central Electricity Research Laboratories, Surrey, UK, 145 (1982).
24. H. Hu, K. Zhou, K. Meng, L. Song and Q. Lin, *Energies*, **10**, 242 (2017).
25. C. H. Pang, B. Hewakandamby, T. Wu and E. Lester, *Fuel*, **103**, 454 (2013).
26. T. F. Wall, S. P. Bhattacharya, D. K. Zhang, R. P. Gupta and X. He, *Prog. Energy Combust. Sci.*, **19**, 487 (1993).
27. A. L. Robinson, S. G. Buckley and L. L. Baxter, *Energy Fuels*, **15**, 66 (2001).
28. A. Y. Al-Otoom, G. W. Bryant, L. K. Elliott, B. J. Skrifvars, M. Hupa and T. F. Wall, *Energy Fuels*, **14**, 227 (2000).
29. J. W. Bang, Y. J. Lee, D. G. Shin, Y. Kim, S. R. Kim, C. S. Baek and W. T. Kwon, *J. Korean Ceram. Soc.*, **53**, 659 (2016).
30. A. Michot, D. S. Smith, S. Degot and C. Gault, *J. Eur. Ceram. Soc.*, **28**, 2639 (2008).
31. J. Bourret, A. Michot, N. Tessier-Dayen, B. Naït-Ali, F. Pennec, A. Alzina, J. Vicente, C. S. Peyratout and D. S. Smith, *J. Am. Ceram. Soc.*, **97**, 938 (2014).
32. J. D. Watt and F. Fereday, *J. Inst. Fuel*, **42**, 99 (1969).
33. H. Namkung, L. H. Xu, T. J. Kang, D. S. Kim, H. B. Kwon and H. T. Kim, *Appl. Energy*, **102**, 1246 (2013).
34. H. Namkung, L. H. Xu, W. C. Shin, T. J. Kang and H. T. Kim, *Fuel*, **117**, 1274 (2014).
35. H. Namkung, T. J. Kang, L. H. Xu, Y. S. Jeon and H. T. Kim, *Korean J. Chem. Eng.*, **29**, 464 (2012).
36. C. L. Senior and S. Srinivasachar, *Energy Fuels*, **9**, 277 (1995).
37. E. Raask, *Mineral impurities in coal combustion, Behavior, Problem and Remedial measure*, Hemisphere Publishing, Washington DC (1985).
38. A. Y. Al-Otoom, L. K. Elliott, T. F. Wall and B. Moghtaderi, *Energy Fuels*, **14**, 994 (2000).
39. http://dspace.mit.edu/handle/1721.1/27224 (access: Oct. 2, 2016).
40. R. W. Bryers, *Factors critically affecting fireside deposits in steam generators*, in: R. P. Gupta, T. F. Wall, L. L. Baxter (Eds.), pp. 105-131, The Impact of Mineral Impurities in Solid Fuel Combustion, Kluwer Academic Press, New York (1999).
41. R. M. German, *Powder metallurgy science*, 2nd Ed., Princeton, New Jersey (1994).
42. R. P. Gupta, T. F. Wall and L. L. Baxter, *The thermal conductivity of coal ash deposits relationships for particulate and slag structures*, in: R. P. Gupta, T. F. Wall, L. L. Baxter (Eds.), pp. 65-84, The Impact of Mineral Impurities in Solid Fuel Combustion, Kluwer Academic Press, New York (1999).
43. T. F. Wall, S. P. Bhattacharya, L. L. Baxter, G. Richards and J. N. Harb, *Fuel Process. Technol.*, **44**, 143 (1995).
44. D. W. Anderson, R. Viskanta and F. P. Incropera, *J. Eng. Gas Turbines Power*, **109**, 215 (1987).
45. K. C. Mills and J. M. Rhine, *Fuel*, **68**, 904 (1989).
46. H. R. Rezaei, R. P. Gupta, G. W. Bryant, J. T. Hart, G. S. Liu, C. W. Bailey, T. F. Wall, S. Miyamae, K. Makino and Y. Endo, *Fuel*, **79**, 1697 (2000).
47. http://www.coaltech.com.au/LinkedDocuments/Slagging%20&%20Fouling.pdf (access : Oct. 10, 2016).